

Range-Coder with fast Adaptation and Table-Based Decoding

Tilo Strutz and Roman Rischke

Abstract—The transmission or storage of signals typically involves data compression. The final processing step in compression systems is generally an entropy coding stage, which converts symbols into a bit stream based on their probability distribution. A distinct class of entropy coding methods operates not by mapping input symbols to discrete codewords (as in Huffman coding) but by operating on intervals or ranges. This approach enables a more accurate approximation of the source entropy, particularly for sources with highly skewed or varying symbol distributions. Representative techniques in this category include traditional arithmetic coding, range coding, and methods based on asymmetric numeral systems (ANS). Due to their near-optimal compression efficiency and flexibility, these interval-based entropy coders are integral to modern data compression systems. The complexity of these methods depends mainly on three processing steps: the core routines of encoding and decoding doing the calculations, the interval-based determination of the correct symbol at decoder, and the efforts of keeping updated with respect to the varying symbol distribution.

The interval-based symbol determination at decoder typically demands for a searching procedure. In previous literature, it could be shown that the search can be replaced by a table-based approach with only $\mathcal{O}(1)$ -complexity but having the side-effect that the adaptation of the symbols statistic becomes infeasible because of the high time-consumption of adapting the table.

We propose an adaptation process using a ring-buffer technique enabling the adaptive table-based decoding procedure as well as the replacement of a division by a bit-shift operation at encoder and decoder core routines. This accelerates the coding process significantly. In static (non-adaptive) mode, the coding time can be reduced by about 40 percent. In adaptive mode, the proposed technique is faster than alternative approaches for alphabets from about 12 to 64 different symbol when comparing the overall encoder+decoder time.

Index Terms—interval-based coding, adaptive coding, arithmetic coding, range coding, ring buffer

I. INTRODUCTION

GENERAL data compression, and video encoding in particular, can be very time-intensive when aiming for both high compression efficiency and excellent data quality. A significant portion of the processing time is often spent searching for optimal parameters. In video coding, this is most evident in the temporal prediction of image content, commonly referred to as motion estimation [1]–[7]. Another crucial step involves selecting the appropriate processing mode [8]–[14]. Detailed analysis also shows that the entropy coding phase can involve computationally expensive procedures [15], [16] and efforts have been made to design efficient structures for hardware implementations [17]–[20].

preprint January 13, 2026

T. Strutz and R. Rischke are with Coburg University, Friedrich-Streib-Straße 2, 96450 Coburg, Germany.

Entropy coding is a core component of any data compression system. It operates by assigning a specific number or fraction of bits to each symbol s_i , based on its given or estimated probability $p(s_i)$. Ideally, the bit allocation reflects the symbols information content, defined as $I(s_i) = \log_2[1/p(s_i)]$.

Interval-based coding methods offer a practical approach towards this symbol-to-bit assignment. One of the earliest and most extensively studied techniques in this category is *arithmetic coding* (AC) [21], which divides a numerical interval into subintervals proportional to the probabilities of the symbols. A closely related method is *range coding* (RC), introduced in the 1970s [22]. Although conceptually similar to arithmetic coding, range coding operates on digits from number systems with arbitrary bases, not limited to binary or decimal. In principle, arithmetic coding can be viewed as a special case of range coding. For practical reasons, range coding typically uses a base of $b = 256$, enabling byte-wise input and output. A third method in this category is based on asymmetric numeral systems (ANS) [23], [24]. Like RC, the range ANS (rANS) variant also processes data in bytes. However, it employs a first-in-last-out mechanism, meaning the encoder must handle data in reverse order compared to the decoder. This reversal introduces complexity in data management, particularly in adaptive coding scenarios [25], [26].

All three interval-based coding techniques are capable of handling multi-symbol alphabets with $K \geq 2$. This capability eliminates the need to convert symbols into binary sequences that require individual probability estimates – an approach used in methods like context-based adaptive binary arithmetic coding (CABAC) [27], [28] and other binary coders [29]–[31] – and can improve the throughput [32].

Efficient coding of large alphabets offers advantages in various applications and remains an active area of research [25], [33]–[38].

These multi-symbol methods have three components in common: (i) the core calculations mapping the probability distribution to a range of numbers where each symbol corresponds to a subinterval, (ii) a procedure that finds the correct symbol regarding a computed internal status value at decoder, and (iii) an adaptation process that creates the symbol distribution and keeps track of its changes.

The symbol distribution has to be related to an array of cumulative counts. As the adaptive coding process typically starts with an assumed flat distribution, the array additionally has to be updated after processing each individual symbol [39]. Moreover, when the distribution changes within the

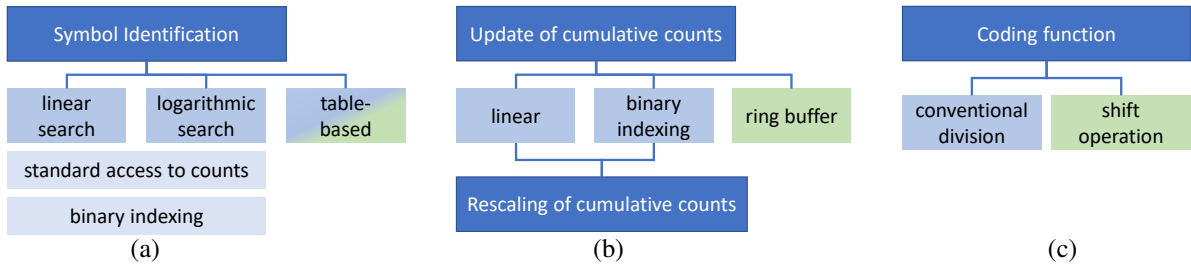


Fig. 1: Methods considered for comparison: (a) search methods for symbol determination in decoder, (b) methods for updating the symbol statistics, (c) methods for symbol coding. Proposed methods are marked in green.

symbol sequence, all counts should be regularly downscaled in order to forget old symbols and up-weighting newly occurring symbols.

The problem of symbol determination at decoder typically involves searching routines which is a time-consuming issue for alphabets with $K \gg 2$. Special strategies to minimise its complexity have been investigated for example in [40]. The searching can only be avoided using a table that maps the internal status value directly to the corresponding symbol. This has been identified in [40] as best option in static compression mode where the symbols distribution remains fixed. However in adaptive processing, not only the cumulative counts must be modified but also the mapping table, which makes this procedure too time-costly, especially after the rescaling of counts.

This paper proposes a new approach that overcomes this problem by using a ring buffer memorizing most recent symbols. This technique additionally allows a special scaling of the symbol counts enabling the substitution of an integer division with a bit-shift operation at both encoder and decoder. This accelerates the core of encoding and decoding.

Figure 1 summarizes the different approaches that are discussed in this paper. One major issue is the symbol identification at the decoder, Figure 1(a). Typically, a search procedure is required. Logarithmic search has a lower \mathcal{O} -complexity than linear search, however this advantage becomes active only if the number of intervals (i.e. the alphabet size) is high enough. In [40] it could already be shown that table-based decoding would be the best option, since it has only $\mathcal{O}(1)$ -complexity. However, in adaptive compression mode, updating the symbol statistics gets very time-consuming making it slower in total. Linear and logarithmic search can be combined with two different adaptation modes. The standard mode updates the statistic linearly ($\mathcal{O}(n)$) and the binary indexing (BI) mode, proposed by [41], updates the statistic logarithmically ($\mathcal{O}(\log(n))$).

We propose the table-based symbol determination in combination with a new ring-buffer-based updating scheme, Figure 1(b). This scheme not only makes rescaling procedures unnecessary but additionally enables faster coding by replacing a division with a shift operation, Figure 1(c). The effectiveness of the new approach will be validated based on simulated test data and real data in comparison to the other listed methods.

In static (non-adaptive) mode, the decoding can be realized using a table-based procedure that maps code values directly to the correct symbol without a time-costly search. However,

TABLE I: Methods that can be combined in a meaningful manner

Mode	Symbol Identification	Shift Operation	Ring Buffer	BI	Label
static	linear search	on/off	-	no	fwd[RingShift]
	log. search	on/off	-	no	log[RingShift]
	table-based	on/off	-	no	tab[RingShift]
adaptive	linear search	off	yes/no	yes/no	fwd[Ring][BI]
	log. search	off	yes/no	yes/no	log[Ring][BI]
	table-based	off	yes/no	yes/no	tab[Ring][BI]
	linear search	on	yes	yes/no	fwdRingShift[BI]
	log. search	on	yes	yes/no	logRingShift[BI]
	table-based	on	yes	yes/no	tabRingShift[BI]

updating this table in adaptive mode has been too costly so far. Using the proposed ring-buffer technique, table-based decoding can now be combined with adaptive processing in an efficient manner.

Table I provides an overview of possible combinations of methods and algorithms. The rightmost column contains the labels used for investigating the performance.

II. BASICS

The coding process operates over an interval $[0; M]$, which is partitioned into K subintervals – each corresponding to one of the K distinct symbols s_i in the alphabet, where $i = 0, 1, \dots, K-1$. The length of each subinterval is proportional to the frequency (the count) $h(s_i)$ or $h[i]$ of the respective symbol. These frequencies determine the boundaries of the subintervals, which are represented by the cumulative counts $h_k[\cdot]$:

$$h_k[i+1] = h_k[i] + h[i] \quad \forall i = 0, 1, \dots, K-1 \quad (1)$$

$$\text{with } h_k[0] = 0 \text{ and } h_k[K] = \text{totalCount}.$$

In this context, $h_k[i]$ represents the lower boundary, and $h_k[i+1]$ the upper boundary of the subinterval assigned to symbol s_i . The symbols probabilities are estimated as relative frequencies $p(s_i) = p[i] = h[i]/M$.

On the decoder side, all three interval-based coding methods share a common principle: a code value c is inferred from the compressed data stream to identify the current subinterval, thereby determining the decoded symbol. To decode, c is compared against the interval boundaries. If $c \in [h_k[i], h_k[i+1]]$, then s_i is the decoded symbol (see Section III). The cumulative counts $h_k[\cdot]$ also reflect the symbol distribution.

In static coding, the symbol statistics are determined once on the encoder side and then transmitted to the decoder. In adaptive coding, the process typically begins with a uniform

Algorithm 1: Determination of the correct symbol index i using linear forward search

```

1: function GETSYMBOLINFORWARD( $K, c, h_k[\cdot]$ )
2:    $i \leftarrow 1$                                  $\triangleright$  start search at first symbol  $s_0$ 
3:   while  $c \geq h_k[i]$  do  $\triangleright$  if not inside the current sub-
   interval ...
4:      $i \leftarrow i + 1$                            $\triangleright \dots$  go to next index
5:   return  $i - 1$ 

```

distribution and $M = K$. Each time a symbol s_i is encoded or decoded, its count $h[i]$ and automatically also M are incremented.

According to Equation (1), when $h[i]$ is increased by one, all cumulative counts $h_k[j]$ for $i < j \leq K$ must also be updated. In the worst case, this means updating all K cumulative values. For large alphabets, this update process can become a performance bottleneck, necessitating more efficient strategies. Unlike symbol search, this adaptation step affects both encoder and decoder, as they must maintain synchronized cumulative counts (see Section V).

In static compression mode, some symbol counts $h[i]$ may be zero, since the set of possible symbols is predefined and known in advance making it clear which symbols can or cannot occur. In contrast, adaptive compression requires all symbol counts to be at least one, ensuring that every potential symbol can be distinguished. This means that in adaptive mode, the cumulative counts $h_k[i]$ must differ, and no subinterval can have zero width.

However, continuously updating the model by incrementing symbol counts can cause the total count $h_k[K] = M$ to grow excessively. If $h_k[K]$ becomes too large, it may interfere with the proper mapping of counts to the internal state variable used in the coding process. To prevent this, a maximum limit must be imposed on $h_k[K]$.

III. SYMBOL DETERMINATION IN DECODER

Identifying the correct symbol in the decoder requires a search procedure that compares a status variable with the boundaries of subintervals. The larger the symbol alphabet, the more subintervals exist and the search can become time-consuming. This section explains three techniques that proved practical relevance in [40]. Figure 1(a) gives an overview.

A. Conventional searching methods

Linear search is the most straightforward approach for a decoder to locate the correct subinterval and determine the corresponding symbol. It works by sequentially comparing the code value c with each interval boundary until the appropriate match is found.

When the search begins with the first symbol, it is known as a linear forward search, (see **Algorithm 1**). This method was introduced in a first practical implementation of source coding as described in [42]. It is particularly efficient when symbols with lower indices have higher probabilities.

The worst-case complexity of $\mathcal{O}(K)$ can be reduced to $\mathcal{O}(\log K)$ by a logarithmic search which is also known as bisection search, see **Algorithm 2**. In this method, each

Algorithm 2: Determination of the correct symbol index i using logarithmic search

```

1: function GETSYMBOLLOGARITHMIC( $K, c, h_k[\cdot]$ )
2:    $bottom \leftarrow 0; top \leftarrow K$   $\triangleright$  outer interval boundaries
3:   repeat
4:      $i \leftarrow (top + bottom) >> 1$   $\triangleright$  interval in the middle
5:     if  $c < h_k[i]$  then
6:        $top \leftarrow i$                                  $\triangleright$  choose lower half
7:     else
8:        $bottom \leftarrow i + 1$                            $\triangleright$  choose upper half
9:     until  $top == bottom$ 
10:     $\triangleright$  stop if no further subdivision is possible
11:   return  $bottom - 1$ 

```

Algorithm 3: Required procedures of table-based search: initialization, mapping

```

1: procedure CREATETABLE( $K, h[\cdot], t[\cdot]$ )
2:    $idx \leftarrow 0, i \leftarrow 0$ 
3:   repeat                                 $\triangleright$  for all symbol indices
4:      $cnt \leftarrow 0$ 
5:     repeat                                 $\triangleright$  write symbol index into table
6:        $t[idx] \leftarrow i, idx \leftarrow idx + 1, cnt \leftarrow cnt + 1$ 
7:     until ( $cnt == h[i]$ )                   $\triangleright$  repeat  $h[i]$  times
8:      $i \leftarrow i + 1$                        $\triangleright$  next symbol index
9:   until  $i == K$ 
10:  return  $t[\cdot]$ 
11:
12: function GETSYMBOLTABLEBASED( $c, t[\cdot]$ )
13:    $i \leftarrow t[c]$ 
14:   return  $i$ 

```

comparison with an interval boundary effectively halves the number of remaining candidates.

B. Table-based searching

The need for an iterative search to locate a specific subinterval can be entirely eliminated by using a precomputed lookup table. This table directly maps each code value c to its corresponding symbol index. To ensure full coverage, the array must have a size of at least the total symbol count $h_k[K]$.

For instance, if there are four distinct symbols (i.e. $K = 4$) with frequencies as shown in the following table

$$\begin{array}{c|cccc} i & 0 & 1 & 2 & 3 \\ \hline h[i] & 2 & 3 & 1 & 4 \end{array},$$

the total count is equal to 10. The code value c is an element of the half-open interval $[0, h_k[K]]$ and the lookup table $t[\cdot]$ would be

$$\begin{array}{c|cccccccccc} c & 0 & 1 & 2 & 3 & 4 & 5 & 6 & 7 & 8 & 9 \\ \hline i = t[c] & 0 & 0 & 1 & 1 & 1 & 2 & 3 & 3 & 3 & 3 \end{array}.$$

Each symbol index i appears exactly $h[i]$ times in the lookup table. The key advantage of this approach is that every code value c can be instantly mapped to its corresponding symbol index i , eliminating the need for iterative searching.

This table-based method was found in [40] to be the best option in static compression mode, where the symbol distribution is determined once beforehand (see **Algorithm 3**, procedure CREATETABLE()) and remains unchanged throughout the process. The lookup operation has a constant time

Algorithm 4: Encoder procedure of range coding

```

1: procedure RCENCODE(status variables,  $h_k[\cdot]$ , symbol  $i$ )
2:    $low \leftarrow low + h_k[i] \cdot (range/h_k[K])$ 
3:    $range \leftarrow h[i] \cdot (range/h_k[K])$ 
4:   while ( $range < b^{m-1}$ ) do
5:      $\triangleright$  as long as current range is too short,
6:      $\triangleright$  i.e. range comprises less than  $m-1$  digits
7:     UPDATELOW(status variables)  $\triangleright$  scale low and
8:      $range \leftarrow range \cdot b$   $\triangleright$  ... output digits if necessary
9:      $range \leftarrow range \cdot b$   $\triangleright$  scale range
10:     $\triangleright$  ... by shifting one digit position
11:   return status variables

```

Algorithm 5: Decoder procedure of range coding

```

1: procedure RCDECODE(status variables,  $h_k[\cdot]$ , symbol  $i$ )
2:    $code \leftarrow code - h_k[i] \cdot (range/h_k[K])$ 
3:    $range \leftarrow h[i] \cdot (range/h_k[K])$   $\triangleright$  narrow the interval
4:   while ( $range < b^{m-1}$ ) do  $\triangleright$  as long current range is too
5:      $\triangleright$  short, i.e. range comprises less than  $m-1$  digits
6:      $code \leftarrow code \cdot b + input$   $\triangleright$  scale and read next digit from
7:      $\triangleright$  stream
8:      $range \leftarrow range \cdot b$ 
9:   return status variables

```

complexity of $\mathcal{O}(1)$, as implemented in Alg. 3, function GETSYMBOLTABLEBASED(). However, this efficiency comes at the cost of high memory usage, since the table must accommodate all possible code values. To manage this, it is advisable to keep the total symbol count $h_k[K]$ within a reasonable limit.

IV. CORE CALCULATIONS IN ENCODER AND DECODER

In this paper, an implementation of a range coder is used for explaining and investigating the proposed approach. **Algorithm 4** shows the core encoding routine. The procedure RCENCODE() requires the status variables ($low, range$), the distribution model ($h[\cdot], h_k[\cdot]$), and the current symbol s_i as input. The variable m is the number of digits that the internal status variable can comprise and b is the basis of the number system used ($b = 256$).

The cumulative probability is represented by $p_k[i] = h_k[i]/h_k[K]$. As in line 2 of procedure RCENCODE() can be seen, the division with the total count $h_k[K]$ is performed first. This unfortunately reduces the accuracy of computation, however in practical implementations, the quotient $range/h_k[K]$ must then be computed only once. The procedure UPDATELOW() is not of interest in this context and will not be discussed further.

At decoder, similar computations take place, **Algorithm 5**. After the symbol has been determined (see Section III), the decoder can modify the status variables in the same manner as the encoder.

The division $range/h_k[K]$ is one of the most time-consuming operation at both encoder and decoder. It is obvious that the division can be replaced by a bit-shift operation $range >> \log_2(h_k[K])$ if the total count $h_k[K]$ is a power of two. However, this contradicts the idea of successive adaptation of symbol counts as explained in Section II. Next section provides a solution to this problem.

Algorithm 6: Simple update of cumulative counts (with $\mathcal{O}(K)$ complexity) after processing of symbol s_i

```

1: procedure UPDATESUMCOUNTS( $K, h_k[\cdot], i$ )
2:   if  $h_k[K] \geq \text{MAX\_TOTALCOUNT}$  then
3:     RESCALESUMCOUNTS( $K, h_k[\cdot]$ )  $\triangleright$  downscale values if needed
4:   repeat
5:      $i \leftarrow i + 1$   $\triangleright$  lower boundary of symbol must kept unchanged
6:      $h_k[i] \leftarrow h_k[i] + 1$ 
7:   until  $i == K$   $\triangleright$  including last entry (totalCount)
8:   return  $h_k[\cdot]$ 

```

V. HANDLING OF CUMULATIVE COUNTS

In adaptive compression mode, the modification of cumulative counts is a matter of both the encoder and the decoder as already mentioned in Section II. We review conventional algorithms for updating the cumulative counts and present a new technique. Afterwards we describe, how the cumulative counts are handled in static compression mode.

A. Linear update of cumulative counts

When cumulative counts are stored sequentially in an array, updates can be performed using a single loop, as illustrated in **Algorithm 6**. This algorithm is straightforward and relies on just a few basic operations. If symbols with higher indices tend to have higher probabilities, the update process requires only a few iterations and can be executed quickly.

However, when lower-indexed symbols are more frequent, the situation reverses, leading to slower performance. In the worst case, the time complexity is $\mathcal{O}(K)$, while for symmetric distributions, the average complexity is approximately $\mathcal{O}(K/2)$. For large alphabets, this update mechanism may become a bottleneck in terms of processing speed, making it necessary to explore more sophisticated solutions.

B. Updating of counts using binary indexing (BI)

A certain addressing technique can handle cumulative counts in a hierarchical manner and reduces the update complexity to $\mathcal{O}(\log(K))$. This comes with the cost of a more complex access to a single value $h_k[i]$.

Binary indexing, also known as binary index tree or Fenwick tree [41], has been reviewed in detail in [40] and a slightly improved algorithm had been reported. We would like to refer the reader to these articles.

When using the binary-indexing technique, the cumulative counts $h_k[\cdot]$ cannot be accessed directly. Instead, dedicated functions are required. Following procedures are available: GETCOUNTBI(), GETSUMCOUNTBI(), GETSYMBOLBI(), GETSYMBOLLOGARITHMICBI(), UPDATESUMCOUNTSBI(), and RESCALESUMCOUNTSBI(). It is important to understand that only UPDATESUMCOUNTSBI() speeds up processing, since it reduces the number of accesses from $\mathcal{O}(K)$ to $\mathcal{O}(\log K)$. All other functions increase the computational load, because the cumulative counts $h_k[i]$ must be calculated as sums based on the binary index tree.

C. Proposed ring-buffer scheme for adaptive coding mode

Conventional adaptation strategies as discussed above accumulate counts until a certain maximum total count is reached.

Algorithm 7: Initialization for adaptive processing

```

1: procedure RCINITADAPTIVEMODEL( $h_k[\cdot]$ ,  $t[\cdot]$ ,  $K$ , total count  $M$ )
2:    $h_k[0] \leftarrow 0$                                 ▷ lower border of entire interval
3:   for ( $i \leftarrow 0$ ;  $i < K$ ;  $i \leftarrow i + 1$ ) do
4:      $h_k[i + 1] \leftarrow h_k[i + 1] + 1$ 
5:   ▷ subintervals have width equal to 1
6:    $ringBufLen \leftarrow M - K$                       ▷ length of ring buffer
7:    $ringBuffer \leftarrow \text{allocateMemory}(ringBufLen)$ 
8:   for ( $i \leftarrow 0$ ;  $i < ringBufLen$ ;  $i \leftarrow i + 1$ ) do
9:      $ringBuffer[i] \leftarrow K$                       ▷ fill ring buffer with a non-symbol value
10:     $ringIdx \leftarrow 0$                             ▷ start with first element of ring buffer
11:    for decoder only:                                ▷
12:       $t[\cdot] \leftarrow \text{allocateMemory}(M)$ 
13:       $idx \leftarrow 0$                                 ▷ start position in table
14:      for ( $i \leftarrow 0$ ;  $i < K$ ;  $i \leftarrow i + 1$ ) do
15:         $count \leftarrow h_k[i + 1] - h_k[i]$           ▷ derive count of symbol
16:        for ( $j \leftarrow 0$ ;  $j < count$ ;  $j \leftarrow j + 1$ ) do
17:           $t[idx + j] \leftarrow i$                       ▷ fill table with current symbol
18:           $idx \leftarrow idx + count$                   ▷ go to region of next symbol
19:      return  $t[\cdot]$ ,  $h_k[\cdot]$ ,  $ringBuffer[\cdot]$ ,  $ringBufLen$ 
20:

```

Algorithm 8: Update of modelling structures for adaptive processing

```

1: procedure RCUPDATEMODEL( $h_k[\cdot]$ ,  $t[\cdot]$ ,  $K$ , symbol  $i$ , desired total
   count  $M$ )
2:    $oldSym \leftarrow ringbuffer[ringIdx]$           ▷ get symbol to be removed
3:    $ringbuffer[ringIdx] \leftarrow i$                   ▷ overwrite with new symbol
4:    $ringIdx \leftarrow ringIdx + 1$                   ▷ go to position of next oldest symbol
5:   if  $ringIdx == ringBufLen$  then
6:      $ringIdx \leftarrow 0$                             ▷ end of array is reached, go to first position
7:   if  $oldSym < i$  then
8:     for ( $j \leftarrow oldSym + 1$ ;  $j \leq i$ ;  $j \leftarrow j + 1$ ) do
9:        $h_k[j] \leftarrow h_k[j] - 1$ 
10:       $t[h_k[j]] \leftarrow j$                         ▷ only at decoder
11:   else
12:     for ( $j \leftarrow i + 1$ ;  $j \leq oldSym$ ;  $j \leftarrow j + 1$ ) do
13:        $t[h_k[j]] \leftarrow j - 1$                   ▷ only at decoder
14:        $h_k[j] \leftarrow h_k[j] + 1$ 
15:   return  $t[\cdot]$ ,  $h_k[\cdot]$ ,  $ringBuffer[\cdot]$ 

```

Then all counts are halved, for example. This introduces a kind of forgetting and newly occurring symbols get automatically a stronger weight, see for example [40]. We propose another method of keeping track of varying probabilities: when the count of a new symbol is incremented then the count of the oldest symbol has to be decremented.

In the beginning, this approach successively stores the processed symbols in a buffer until the total count $h_k[K]$ reaches a desired value $M = 2^p$. The purpose of M being a power of two had been explained in Section IV.

Since the coding process must start with an initialised array of cumulative counts, i.e. $h_k[j] > h_k[i] \forall j > i \geq 0$, the required buffer size is only $M - h_k[K]$. Typically the process starts with counts $h[i] = 1 \forall i$ leading to $h_k[K] = K$. Therefore, if $M - K$ symbols have been processed, the buffer should be completely filled and the total count $h_k[K]$ is a power of two. Now, the coding procedures (Alg. 4 and 5) can switch from the conventional division operation to the bit-shift operation.

Algorithm 7 depicts the initialization of the ring buffer and the mapping table. During the coding process, both arrays, $ringbuffer[\cdot]$ and $t[\cdot]$, have to be updated. **Algorithm 8** shows the required steps. The oldest symbol is extracted from the ring buffer as it influences the modification of the cumulative counts. Then it is overwritten by the current symbol and the ring-buffer pointer $ringIdx$ is moved to the next position. Now, the count of the removed symbol has to be decremented

and the count of the new symbol has to be incremented. The required modifications of the array of cumulative counts depend on the order of these two symbols. If the old one has a lower index, its upper bound must be decremented (i.e. its count gets smaller) and the lower bound of the new symbol must be decremented (its count gets higher). All values $h_k[j]$ in between are also decremented in order to keep all other interval widths the same. In contrast, if the new symbol i has the lower index, all lower bounds from $i + 1$ up to the old symbol are incremented, leading to an increased count of the new and a decreased count of the old symbol, while keeping all other counts untouched. In ideal case, the new symbol is equal to the old one and nothing has to be changed.

It can be shown that for flat distributions the average number of modifications is only $K/3$ instead of $K/2$ when using Algorithm 6, see Appendix A1. This could be verified by counting the accesses during the coding process. If the distribution is skewed, the computational load is even lower, regardless to which side it is skewed. The geometric distribution used in the investigations (Section VI) demands only about $0.09 \cdot K$ accesses on average while the standard approach requires $0.09 \cdot K$ or $0.91 \cdot K$ depending to which side the distribution is skewed, see Appendix A2.

As the ring buffer had been initialized with values K , the total count $h_k[K]$ increases until the buffer is completely filled and automatically stays fixed afterwards.

From an engineers perspective, the adaptation of the symbols distribution can be interpreted as a kind of filtering. The conventional increment-and-rescale technique corresponds to a filter with infinite impulse response, because the influence of symbols is repeatedly downscaled (until its count equals zero) but not immediately removed. The proposed ring-buffer technique can be seen as a kind of moving-average filter with finite impulse response, where the distribution is solely derived from symbols within a certain window.

D. Proposed procedure in static coding mode

In static processing mode, we neither have to care about updating the array of cumulative counts nor the mapping table. The only point to be discussed here for improving the efficiency of the range coder is to replace the division with a shift operation, as already suggested in Section IV.

To achieve this, the symbol distribution must first be derived from the input sequence by counting the occurrences of each symbol. Afterwards, the counts need to be scaled so that the total count matches the desired target value $M = 2^p$, **Algorithm 9**.

The relation of the original total count $h_k[K]$ and the desired value M is used as scaling factor for all symbol counts $h[i]$. In this process, it must be avoided that counts of existing symbols are rounded to zero after downscaling. When the sum of all resulting counts is higher than M , counts of arbitrary symbols are decremented as long as they are not reduced to zero. If the scaling procedure led to a value that is smaller than M , the counts of arbitrary existing symbols are incremented until the current total count matches M . Afterwards all cumulative counts have to be re-computed.

Algorithm 9: Scaling of the symbol distribution to the desired total count

```

1: procedure RSCALEMODEL( $h[\cdot]$ ,  $h_k[\cdot]$ ,  $K$ , desired total count  $M$ )
2:    $scale \leftarrow h_k[K]/M$                                  $\triangleright$  floating-point operation
3:    $currTotCount \leftarrow 0$                                  $\triangleright$  current total count
4:   for ( $i \leftarrow 0$ ;  $i < K$ ;  $i \leftarrow i + 1$ ) do
5:      $count \leftarrow \text{round}(scale \cdot h[i])$ 
6:     if  $h[i] > 0$  then                                 $\triangleright$  if original count was non-zero ...
7:       if  $count == 0$  then
8:          $h[i] \leftarrow 1$                                  $\triangleright \dots$  than keep it non-zero
9:       else
10:         $h[i] \leftarrow count$ 
11:         $currTotCount \leftarrow currTotCount + h[i]$ 
12:    $idx \leftarrow 0$   $\triangleright$  modify single counts until the desired value  $M$  is
13:   reached
14:   while  $currTotCount > M$  do
15:     if  $h[idx] > 1$  then                                 $\triangleright$  only if there is something do decrement
16:        $h[idx] \leftarrow h[idx] - 1$ 
17:        $currTotCount \leftarrow currTotCount - 1$ 
18:      $idx \leftarrow idx + 1$ 
19:     if  $idx == K$  then
20:        $idx \leftarrow 0$                                  $\triangleright$  scan counts again
21:     while  $currTotCount < M$  do
22:       if  $h[idx] > 0$  then                                 $\triangleright$  increment only counts of existing symbols
23:          $h[idx] \leftarrow h[idx] + 1$ 
24:          $currTotCount \leftarrow currTotCount + 1$ 
25:        $idx \leftarrow idx + 1$ 
26:       if  $idx == K$  then
27:          $idx \leftarrow 0$                                  $\triangleright$  scan counts again
28:        $h_k[0] \leftarrow 0$                                  $\triangleright$  re-compute cumulative counts
29:     for ( $i \leftarrow 0$ ;  $i < K$ ;  $i \leftarrow i + 1$ ) do
30:        $h_k[i+1] \leftarrow h_k[i] + h[i]$ 
31:   return  $h_k[\cdot]$ ,  $h[\cdot]$ 

```

The counts must be transmitted to the decoder and then both, encoder and decoder, are able to use the shift-operation-based coding routines.

E. Remarks regarding the table-based decoding method

In adaptive coding mode of table-based searching, subsection III-B, not only the array of cumulative counts has to be updated, as described in Subsections V-A and V-C, but additionally the mapping table $t[\cdot]$ has to be modified after each individual symbol has been processed. Since this table has the size of $h_k[K]$, this modification seems to be very time-consuming. However, if one examines how the mapping table changes when a single symbol s_i with a certain index i has been processed, it becomes obvious that the modification complexity in the worst case is only $\mathcal{O}(K)$ instead of $\mathcal{O}(h_k[K])$ [40]. Looking at the toy example above, let us assume that the count of s_1 has been incremented from 3 to $h[1] = 4$. The mapping table must then be changed to

c	0	1	2	3	4	5	6	7	8	9	10
$i = t[c]$	0	0	1	1	1	1	2	3	3	3	3

It can be seen that only $K - i = 4 - 1 = 3$ table entries have been changed, namely at $c = 5, 6$, and 10. These are the positions of the interval boundaries. Therefore, only K entries need to be accessed in the worst case ($K/2$ on average for flat distributions) and the update complexity is indeed $\mathcal{O}(K)$. Procedure **UPDATETABLE()** in **Algorithm 10** shows the corresponding pseudo-code.

Although this table-update process is quite efficient, its worst-case complexity is still $\mathcal{O}(K)$ and has to be added

Algorithm 10: Update of cumulative counts for table-based method

```

1: procedure UPDATETABLE( $K$ ,  $t[\cdot]$ ,  $h_k[\cdot]$ ,  $i$ )
2:   repeat
3:      $idx = h_k[i + 1]$                                  $\triangleright$  position to be changed
4:      $t[idx] \leftarrow i$                                  $\triangleright$  set new symbol index  $i$ 
5:      $i \leftarrow i + 1$                                  $\triangleright$  go to next symbol index
6:   until  $i == K$ 
7:   return  $t[\cdot]$ 

```

to complexity of updating the cumulative counts. Ideally, the table modification can be done in the same processing loop in which also the cumulative counts are updated reducing some overhead in computation.

When using the ring-buffer approach proposed in Section V-C, the update of the mapping table can be handled simultaneously with updating the cumulative counts (Alg. 8, lines 10 and 13) and requires less efforts than in Alg. 10.

VI. INVESTIGATIONS AND RESULTS

All investigation are based on the authors implementation of a range coder with a number basis of $b = 256$. The precision of the coding engine is set to six digits, i.e. 48 bits in total. The modelling of data distribution uses a total count of $M = 2^{12}$ per default. This means, if the alphabet size is $K = 32$, for example, the maximum count per symbol would be $2^{12-5} = 128$ for a uniform distribution.

A. Methodology

All simulations were conducted using a range coder implemented in ANSI-C, integrated with various algorithmic approaches. The programs were executed on a notebook equipped with an Intel i7-1165G7 2.80GHz processor. To measure execution times, we used the `__rdtsc()` function, which returns the processor's time stamp counter representing the number of clock cycles since the last system reset [43]. Two time stamps were recorded: one immediately before the data encoding begins (including the setup of all necessary arrays for modelling), and another right after all symbols have been processed. The difference between these two values is taken as the time measurement. It is important to note that all input and output data were handled in memory. Consequently, file I/O operations such as reading from or writing to disk were excluded from the timing measurements.

The measured execution time does not necessarily correspond to the actual number of CPU instructions executed during the coding process. Two key factors must be considered. First, the CPU may be concurrently handling other background tasks, which can affect timing accuracy. Second, the execution time is influenced by the CPU's clock frequency, which is not constant. Modern processors can dynamically adjust their clock speed boosting performance during short, intensive workloads. However, under sustained high loads, such as in our simulations, the CPU temperature may rise significantly, triggering thermal throttling. This mechanism reduces the clock frequency to prevent overheating, and it remains in effect until the temperature drops below a safe threshold. As a result, the CPU frequency can fluctuate frequently, making

Algorithm 11: Procedure of generating a sequence with geometrically distributed symbols

```

1: procedure GENGEOMETRIC(length of sequence N, alphabet size K,  

   parameter k)
2:    $p \leftarrow 2^{-1/2^k}$                                 define probability based on k
3:   for  $i = 0 : K - 1$  do                         compute single probabilities
4:      $\lfloor pr[i] \rfloor \leftarrow (1 - p) \cdot p^i / (1 - p^K)$ 
5:    $prSum[0] \leftarrow 0$                                 compute cumulative probabilities
6:   for  $i = 0 : K - 1$  do
7:      $\lfloor prSum[i + 1] \rfloor \leftarrow prSum[i] + pr[i]$ 
8:   arr[.]  $\leftarrow$  array with N uniformly distributed values
9:    $\in [0; 1)$ 
10:  for  $n = 0 : N - 1$  do                         for all sequence elements
11:     $i \leftarrow 0$ 
12:    while arr[ $n$ ]  $\geq prSum[i + 1]$  do
13:       $i \leftarrow i + 1$                                 search corresponding symbol
14:    sequence[ $n$ ]  $\leftarrow i$ 
15:  return sequence[..]

```

time-based measurements unreliable indicators of actual computational effort.

To minimize the impact of background processes, all unnecessary applications were closed, the internet connection was disabled, and each measurement was repeated five times, with the lowest value selected for analysis. The issue of fluctuating CPU frequency was addressed by limiting the maximum processor performance to 75% via the Windows 11 power settings. This adjustment resulted in a nearly constant CPU frequency of approximately 2.0 GHz, as confirmed through the task manager.

The experiments use ten data sequences, each comprising 10^8 symbols [44]. The sequences differ in the number of the alphabet size, which is chosen as $K = 2^n$ with $n = 1, 2, \dots, 10$. As the algorithm performance usually depends on the symbol distribution, two typical variants are taken into account: uniform (flat) distribution with $p(s_i) = 1/K \forall i$ and truncated geometric distribution with

$$p(s_i) = \frac{(1 - p) \cdot p^i}{1 - p^K}, \quad p = 2^{-1/2^k}, \quad i = 0, 1, \dots, K-1. \quad (2)$$

This type of distribution has already been used by others, e.g. [40], [45], and is representative for a large class of data. The generating process is shown in **Algorithm 11**.

The parameter k was selected such that the probability of symbols decreases significantly with increasing i and the symbol counts remain above zero:

$$k(K) = \max(0, \lfloor \log_2(K) \rfloor - 4). \quad (3)$$

B. Static processing mode

The static mode determines the symbol distribution in a preprocessing step by counting all symbols once. This statistic remains fixed for all symbols to be processed. Thus on encoder side, only the influence of the shift operations on the processing speed can be investigated. On decoder side, also the algorithm for symbol identification has an impact.

1) *Uniform distribution*: **Figure 2** presents the number of clocks per symbol determined in dependence on the symbol alphabet when coding symbols with equal probabilities. The labels are chosen according Table I. Since ‘fwd’, ‘log’, and ‘tab’ discriminate between different algorithms for symbol

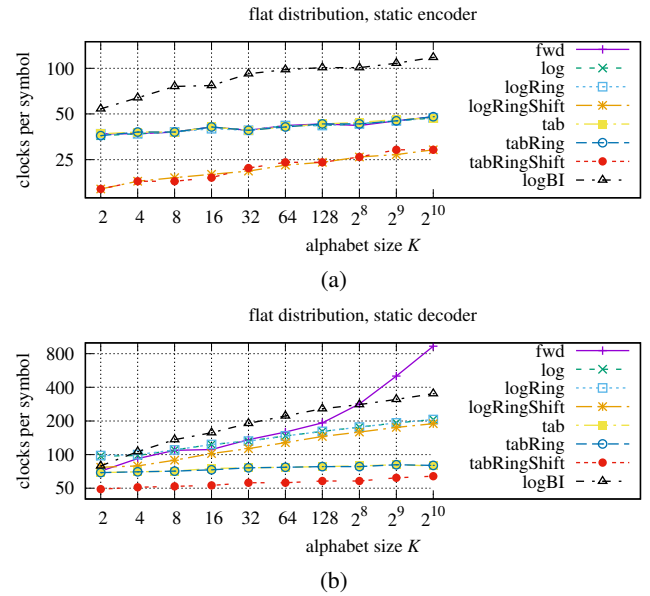


Fig. 2: Required processor clock cycles per symbol dependent on the alphabet size: flat distribution, $h(s_i) = h(s_j) \forall (i, j)$: (a) encoder, (b) decoder

determination at decoder, they have no influence on the encoder and the curves are in principle identical in Figure 2(a). Sub-label ‘Ring’ refers to the adaptation process and also has no impact if operation in static mode. The only discrimination in this investigation tangents the substitution of a division by a bit-shift operation. It saves about 20 clocks per symbol corresponding to a reduction by 40% - 50% at the encoder. Additionally, the binary indexing scheme ‘logBI’ has been investigated. It performs worst, since the hierarchical structure of storing the cumulative counts generates overhead when accessing the values.

The curves in Figure 2(b) showing the behaviour of the decoder are a bit more diverse. Table-based symbol determination has almost constant processing times regardless the alphabet size because its complexity is $\mathcal{O}(1)$, see explanations to Alg. 3. The ring buffer is required for adaptation only, therefore the results of ‘log’ and ‘logRing’ and also for ‘tab’ and ‘tabRing’ are the same.

2) *Geometric distribution*: The results of time measurement when compression the data with geometric distribution are shown in **Figure 3**. The encoder curves are about the same compared to the experiments with uniform distributions. The encoding process solely gets a little bit slower. At decoder side, the linear forward search can benefit from the distribution that is skewed towards symbols with small indices. The proposed method ‘tabRingShift’ is the clear winner when operating in static mode.

C. Adaptive processing mode

Using the same data sets, the investigation were repeated, running the encoding/decoding software in adaptive mode. The coding times now additionally depend on the adaptation method.

In conventional adaptation mode, the software starts with a uniform distribution and, after processing each symbol, its

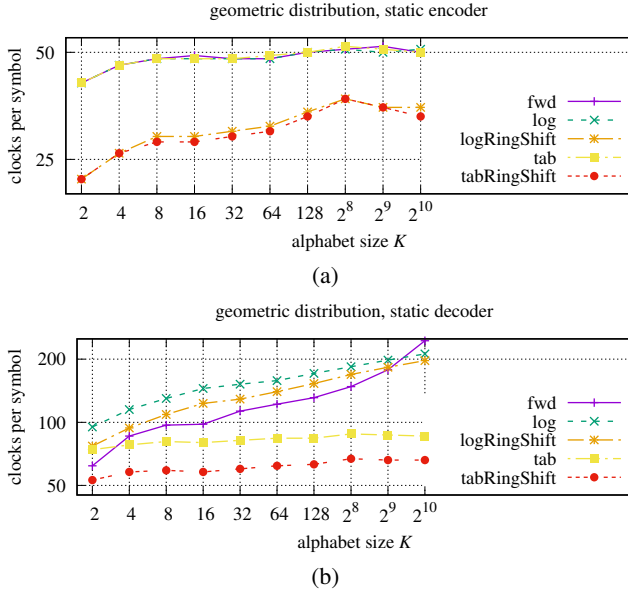


Fig. 3: Required processor clock cycles per symbol dependent on the alphabet size K for geometric symbol distributions: (a) encoder, (b) decoder

count is incremented. When a total count of 2^{12} is reached, all counts are downscaled by factor 2. The proposed adaptation mode utilizes a ring buffer of size $2^{12} - K$. As long as the buffer is not yet completely filled, the behaviour is like in the conventional mode. Then, the total count remains fixed, since the increment of a new symbol's count is combined with the decrement of the oldest symbol's count. This is also the moment were the coding routines replace the division by the shift operation.

The second option is using the binary indexing that allows updating the cumulative counts with $\mathcal{O}(\log K)$ instead of $\mathcal{O}(K)$.

1) *Uniform distribution*: Fig. 4 shows the results for the encoder and decoder processes when applied to a flat distribution. The computational load is now dominated by the adaptation of the cumulative counts. In encoder, the conventional linear update (UPDATESUMCOUNTS()), which is used in combination with 'fwd' and 'log', seems to be preferable up to an alphabet size of $K = 32$. The ring-buffer-based adaptation (RCUPDATEMODEL()) is not very competitive in this range. Albeit there are less accesses to the array of cumulative counts when using the ring-buffer technique, the overhead of updating the ring buffer itself seems to slow down the processing. Beyond $K = 32$, the benefits of the binary-indexing method apply.

At decoder side, ring-buffer adaptation and shift operation in combination with the very fast table-based symbol determination make the proposed scheme 'tabRingShift' the best choice for alphabets with $K < 128$. For larger alphabets, the logarithmic symbol determination in combination with ring-buffer-based adaptation seems to be favourable. Probably, updating the table gets too costly for larger alphabets.

2) *Geometric distribution*: When processing geometric distributions, the behaviour is similar to uniform distribution, Fig. 5. Most algorithms can utilize the skewed distribution

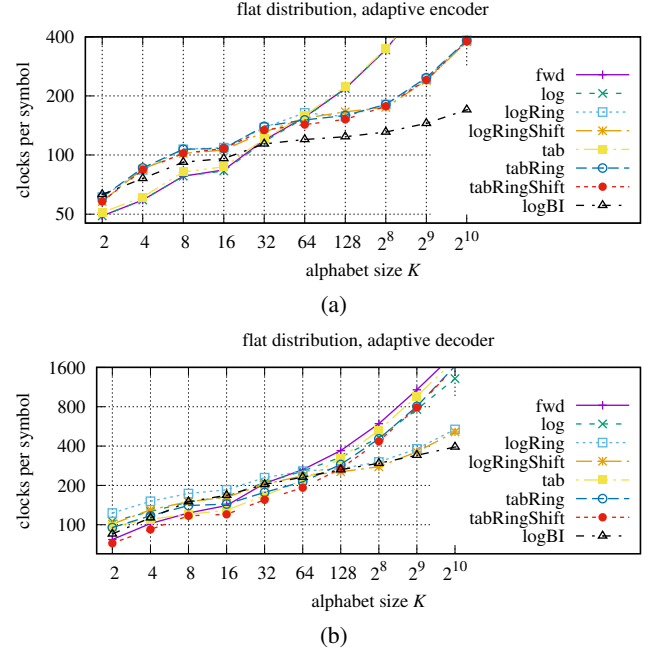


Fig. 4: Adaptive mode comparison for uniform distribution: (a) encoder, (b) decoder

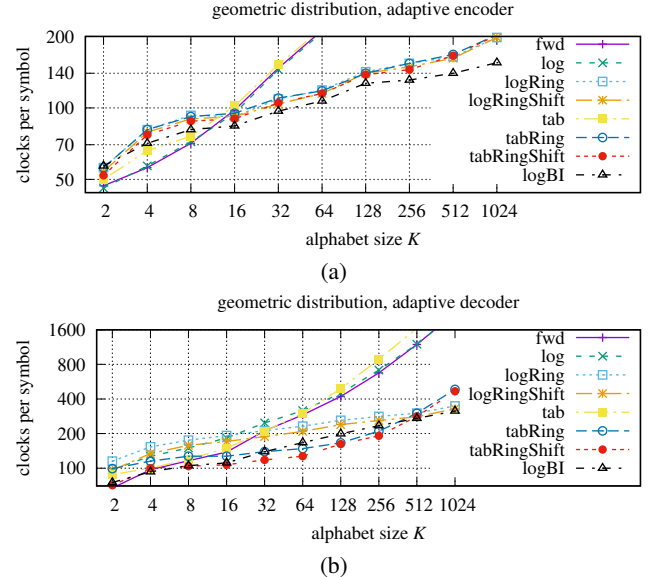


Fig. 5: Adaptive mode comparison for geometric symbol distribution: (a) encoder, (b) decoder

for faster processing. Only the linear update of cumulative counts has now a steeper curve, since on average more than $K/2$ cumulative counts have to be incremented per symbol.

D. Influence of binary indexing

The remaining question to answer is, whether the advantages of table-based decoding and ring-buffer adaptation can be combined with the benefits of binary indexing.

Using a ring buffer provides the advantage that not all cumulative counts starting from the current symbol up to the end of the array have to be accessed. Instead, only the elements

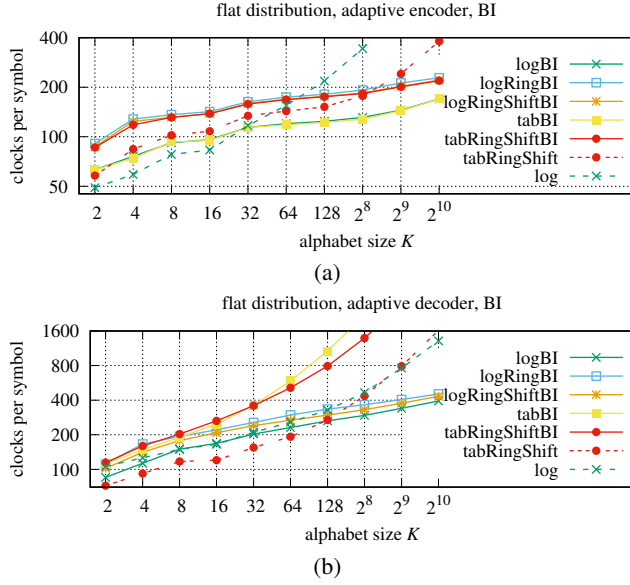


Fig. 6: Adaptive mode comparison for uniform symbol distribution when using binary indexing: (a) encoder, (b) decoder

between the new and the old symbol (which is overwritten by the new) must be modified. However, the binary index tree does not support such a range modification. The cumulative counts have first to be incremented according the new symbol and afterwards they have to be decremented according to the old symbol. The big-O complexity is still $\mathcal{O}(\log K)$, but the efforts have doubled.

A second problem arises if the table-based decoding is activated. In standard mode, the cumulative counts and the mapping table can be modified in a single loop. When using the binary indexing there is no such synergy effect and efforts of updating both arrays simply sum up.

Figure 6 illustrates this set of problems for uniform distributions. The curves for approaches applying the binary indexing have the same colours and point types as before, only the lines are drawn as solid lines. For comparison, also the best results without binary indexing are shown. The encoder significantly benefit from BI for $K \geq 32$, Fig.6(a). For smaller alphabets the standard addressing is faster. The combination of BI with ring-buffer adaptation ('logRingBI') slows the processing down for reasons already explained above. The options 'log' versus 'tab' refer to the symbol identification in decoder, thus the curves should be identical.

The decoder plots, Figure 6(b), shows a slightly different picture. The proposed approach 'tabRingShift' without BI performs best for $K \leq 128$. The combination of BI and table-based decoding dramatically increase the adaptation costs making it impossible to benefit from their advantages.

The investigations based on the datasets with geometric distribution of symbols lead to similar results, whereas 'tabRingShift' benefits most from this skewed distribution, **Figure 7**.

E. Comparison of different settings

Tab. II provides a rough overview of the best choice given a

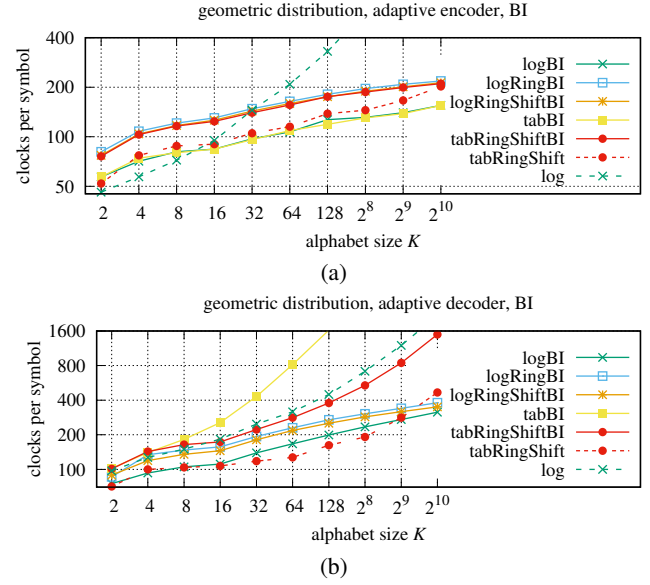


Fig. 7: Adaptive mode comparison for geometric symbol distribution when using binary indexing: (a) encoder, (b) decoder

certain application mode and data type. The proposed approach with table-based decoding and substitution of a division with a bit-shift operation performs fastest in static compression mode. In adaptive mode, these two features can be enabled by the proposed adaptation of cumulated counts using the ring-buffer approach. On decoder side, this is the best option for alphabet sizes to about $K = 80$ (uniform symbol distribution) or $K = 500$ (geometric distribution).

On encoder side, there is no advantage of fast table-based processing. The adaptation of cumulated counts dominates the time-consumption here. Dependent on the symbol's distribution, the standard linear adaptation is favourable up to $K = 32$ or $K = 12$, respectively. Maintaining the ring buffer takes to much efforts in relation. For larger alphabets, the logarithmic complexity of the binary-indexing technique allows faster modifications. This also can be observed for the decoder, where BI becomes an option for about $K \geq 81$.

The problem is, that encoder and decoder must apply the same adaptation strategy to be compatible: either both use the ring buffer or both do not. If the application demands either for fast encoding or decoding, Table II can be used for guidance. If the overall time consumption is important, we have to investigate the sum of encoder and decoder times, **Figure 8** and rightmost column in Table II. It can be seen that the proposed 'tabRingShift' approach is a good compromise for alphabets with $K \leq 128$ (flat) or $K \leq 256$ (geometric) different symbols, respectively.

F. Investigation of the ring-buffer approach

1) *Influence of the ring-buffer size*: The size $M - K$ of the ring-buffer array influences two things: (i) the number of symbols to be processed before the algorithm can switch from division to bit-shift operation and (ii) how precise the cumulative counts $h_k[\cdot]$ can represent the cumulative probabilities $p_k[\cdot]$. **Figure 9** shows the difference between the achieved

TABLE II: Recommended settings for different alphabet sizes. Labels are explained in Table I

K	Encoder		Decoder		Encoder + Decoder	
	static	adaptive flat geom.	static	adaptive flat geom.	adaptive flat geom.	adaptive flat geom.
~ 2 ... 12	tabRingShift	log	tabRingShift	tabRingShift	tabRingShift	fwd
~ 13 ... 32	tabRingShift	log	tabRingShift	tabRingShift	tabRingShift	tabRingShift
~ 33 ... 80	tabRingShift	logBI	tabRingShift	tabRingShift	tabRingShift	tabRingShift
~ 81 ... 500	tabRingShift	logBI	tabRingShift	tabRingShift	tabRingShift	logBI
~ 501 ... 1024	tabRingShift	logBI	tabRingShift	logBI	tabRingShift	logBI

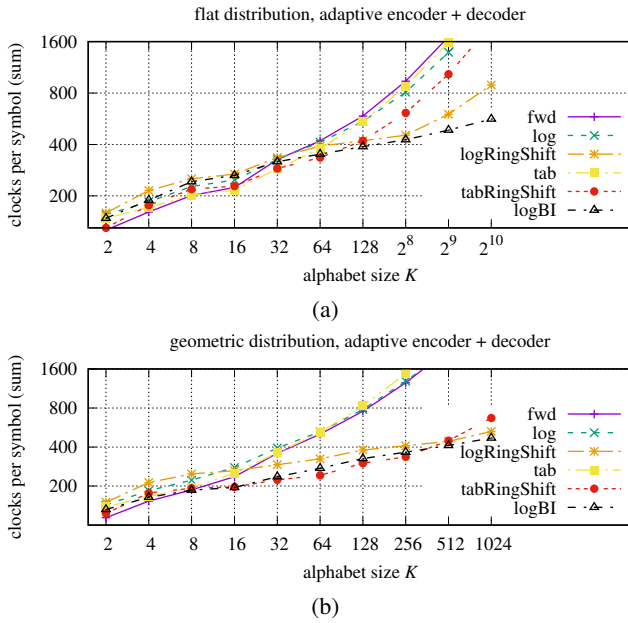
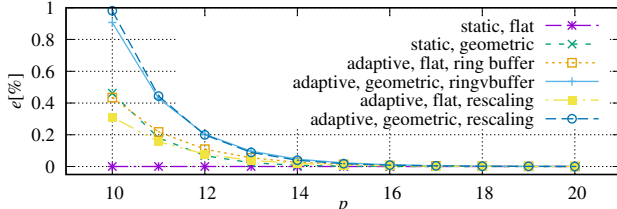


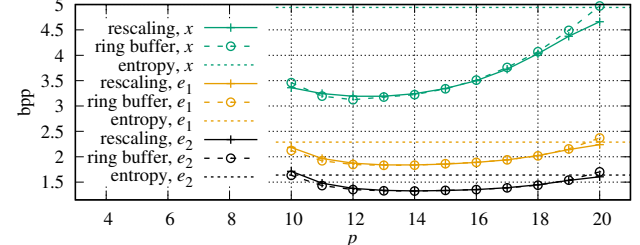
Fig. 8: Total processing times (encoder+decoder): (a) uniform distribution, (b) geometric distribution

Fig. 9: Accuracy of entropy coding in terms of difference between bitrate and signal entropy $e = 100 \cdot (R - H)/H$ [%] dependent on the chosen total count $M = 2^p$

bitrate (number of compressed per encoded symbol) and the signal entropy H for the ring-buffer approach in comparison to the standard approach with periodic rescaling of cumulative counts. The datasets with $K=32$ different symbols have been exemplary chosen to investigate the performance.

The static mode can perfectly match the uniform distribution with an entropy of $H = 5.0$ bit/symbol as this distribution could be represented with counts of only $h[i] = 1 \forall i$. The more non-uniform a distribution is, the more precise the probabilities should be. The chosen geometric distribution has an entropy of $H = 2.978335$ bit/symbol. It can be seen that the achieved bitrate deviates from the entropy by about 0.1% if less than $p = 13$ bits are used for the entire interval.

In adaptive mode, the distribution model relies on only

Fig. 10: Compression efficiency of ring-buffer and rescaling adaptation dependent on the chosen total count $M = 2^p$ for test images x , e_1 , and e_2

$M - K$ symbols which can be simultaneously stored in the ring buffer. Also here, the real distribution is not ideally represented, if the precision is too low.

2) *Application to real data with varying statistics:* In real data, symbol probabilities often vary depending on which part of the symbol sequence is in focus. Also here we investigate the compression efficiency of ring-buffer adaptation in comparison to conventional increment-and-rescale adaptation. Three images have been chosen which were already used as test data in [25], see [44]. Image x is an RGB image containing screen content, while images e_1 and e_2 are both prediction error images of x created by different prediction methods. The images are stored as raw data in planar mode RRR..GGG..BBB. **Figure 10** shows the results for image x . The entropy $H(x) = 4.942$ bit/pixel of this image is drawn as a straight dotted line. Both ring-buffer and rescaling adaptation are able to compress the image with less bits per pixel (bpp) since the symbol distribution is drawn from a local context when using these adaptation techniques. The optimum (lowest bitrate) seems to be around $M = 2^{12}$ for both approaches.

The two prediction error images have originally lower entropies and adaptive coding including forgetting of old symbols facilitates saving at even lower bitrates.

VII. SUMMARY

Interval-based coding methods like conventional arithmetic coding, range coding, and range ANS require three time-consuming processing steps: the symbol search at the decoder, the core calculations at encoder and decoder, and, when operating in adaptive mode, the adaptation of cumulative counts at encoder and decoder.

We presented a new adaptation approach which can be used in conjunction with the very fast table-based symbol determination at decoder. It is based on storing the most recent symbols in a ring buffer. If the size of this buffer is appropriately chosen, the total sum of all counts can be

kept constant equal to a power of two. This facilitates the substituting of a division with a bit-shift operation at both, encoder and decoder.

The performance of the proposed scheme has been investigated in comparison with other promising approaches by carrying out practical simulations. The investigations included different alphabet sizes $2 \leq K \leq 1024$, flat and geometric symbol distribution, and two modes of operation (static and adaptive). It could be shown that replacing an integer division by a shift operation saves about 40% of computation load. Further more, the proposed approach is faster than alternative methods in static compression. Even in adaptive compression mode, where updating the symbol statistic creates the major payload, the proposed scheme performs among the best approaches. Only if the number of different symbols becomes too large, accessing the cumulative counts via binary indexing excels the proposed scheme.

APPENDIX

A. Number of accesses to array of cumulative counts

Given an array of K elements, we are interested in the average number of accesses that are required to update the array content.

1) *Assumed uniform distribution of symbols*: The conventional approach gets an index $i \in [0; K)$ as input and requires to access all elements from $i + 1$ to K , thus the number of accesses is $x = K - i$. If i follows a uniform distribution, the expectation value of x is

$$\begin{aligned} E[X] &= \frac{1}{K} \cdot \sum_{i=0}^{K-1} K - i = \frac{1}{K} \cdot \left[K^2 - \sum_{i=0}^{K-1} i \right] \\ &= \frac{1}{K} \cdot \left[K^2 - \frac{(K-1)K}{2} \right] = K - \frac{K-1}{2} \approx \frac{K}{2}. \end{aligned} \quad (4)$$

The proposed ring-buffer approach uses two indices $i \in [0; K)$ and $j \in [0; K)$ as input and requires to access all elements from i to j , thus the number of accesses is $d = |j - i|$. There are exactly $2 \cdot (K - d)$ pairs (i, j) . If i and j follow a uniform distribution, the expectation value of d over all possible K^2 pairs is

$$\begin{aligned} E[D] &= \frac{1}{K^2} \cdot \sum_{d=0}^{K-1} 2 \cdot (K - d) \cdot d = \frac{2}{K^2} \cdot \left[K \sum_{x=0}^{K-1} d - \sum_{d=0}^{K-1} d^2 \right] \\ &= \frac{2}{K^2} \cdot \left[K \frac{(K-1)K}{2} - \frac{(K-1)K(2K-1)}{6} \right] \\ &= (K-1) - \frac{(K-1)(2K-1)}{3K} \\ &= -\frac{3K(K-1) - (K-1)(2K-1)}{3K} = \frac{K^2 - 1}{3K} \approx \frac{K}{3}. \end{aligned} \quad (5)$$

2) *Assumed geometric distribution of symbols*: Symbols i following an unbounded geometric distribution have a probability of $P(i=n) = (1-p) \cdot p^n$. This unbounded (not truncated) distribution is used for simplifying the derivations and provides an upper bound of the average number of accesses.

In conventional approach, all elements from $i + 1$ to K must be modified. Assuming that symbols with highest index ($i = K - 1$) have the highest probability, the average number of accesses x can be approximated by the expectation value of the geometric distribution:

$$E[X] \approx \frac{p}{1-p}. \quad (6)$$

In the typical case however, symbols with low indices have the highest probability and the average number of accesses is about $K - E[X]$.

Using the ring-buffer approach, the distance between two indices i and j (= number of accesses) can be expressed as $d = |i - j| = i + j - 2 \cdot \min(i, j)$. So, the expected distance is

$$E[D] = 2 \cdot E[i] - 2 \cdot E[\min(i, j)] = \frac{2 \cdot p}{1-p} - 2 \cdot E[\min(i, j)]. \quad (7)$$

According to the tail-sum formula, the expectation value of the minimum can be expressed as

$$E[\min(i, j)] = \sum_{n=1}^{\infty} P(\min(i, j) \geq n). \quad (8)$$

It is further assumed that i and j are independent and identically distributed. Then the probability that $\min(i, j)$ is not smaller than n is

$$\begin{aligned} P(\min(i, j) \geq n) &= P(i \geq n \wedge j \geq n) = P(i \geq n) \cdot P(j \geq n) \\ &= P(i \geq n)^2 = p^{2n}. \end{aligned} \quad (9)$$

So, we can formulate (7) using (8) as

$$\begin{aligned} E[D] &= \frac{2 \cdot p}{1-p} - 2 \cdot \sum_{n=1}^{\infty} p^{2n} = \frac{2 \cdot p}{1-p} - 2 \cdot \frac{p^2}{1-p^2} \\ &= \frac{2 \cdot p \cdot (1+p)}{(1-p)(1+p)} - 2 \cdot \frac{p^2}{(1-p)(1+p)} = \frac{2p}{1-p^2}. \end{aligned} \quad (10)$$

This average distance $E[D]$ or number of accesses depends on probability p , Equation (2), which itself depends on the parameter k , see (3). The actual complexity with respect to the investigated alphabet size K is shown in **Table III**.

For large K , these values provide a good approximation of the complexity. For $K \leq 8$, the actual average number of accesses is lower, since d cannot be arbitrarily high for the truncated distribution used.

REFERENCES

- [1] S.-G. Jeong, C. Lee, and C.-S. Kim, “Motion-compensated frame interpolation based on multihypothesis motion estimation and texture optimization,” *IEEE Transactions on Image Processing*, vol. 22, no. 11, pp. 4497–4509, 2013.
- [2] L. Jia, C.-Y. Tsui, O. C. Au, and K. Jia, “A new rate-complexity-distortion model for fast motion estimation algorithm in HEVC,” *IEEE Transactions on Multimedia*, vol. 21, no. 4, pp. 835–850, 2019.
- [3] L. Zhao, S. Wang, X. Zhang, S. Wang, S. Ma, and W. Gao, “Enhanced motion-compensated video coding with deep virtual reference frame generation,” *IEEE Transactions on Image Processing*, vol. 28, no. 10, pp. 4832–4844, 2019.
- [4] H. Meuel and J. Ostermann, “Analysis of affine motion-compensated prediction in video coding,” *IEEE Transactions on Image Processing*, vol. 29, pp. 7359–7374, 2020.
- [5] F. Bossen, K. Sühring, A. Wieckowski, and S. Liu, “VVC complexity and software implementation analysis,” *IEEE Transactions on Circuits and Systems for Video Technology*, vol. 31, no. 10, pp. 3765–3778, 2021.
- [6] Y. Liu, M. Abdoli, T. Guionnet, C. Guillemot, and A. Roumy, “Statistical analysis of inter coding in VVC test model (VTM),” in *2022 IEEE Int. Conference on Image Processing (ICIP)*, 2022, pp. 3456–3459.
- [7] Y.-G. Chou and J.-J. Chen, “H.266/VVC time complexity reduction by learned models and image statistical features,” in *2023 IEEE International Conference on Visual Communications and Image Processing (VCIP)*, 2023, pp. 1–5.
- [8] X. Cai and J. S. Lim, “Algorithms for transform selection in multiple-transform video compression,” *IEEE Transactions on Image Processing*, vol. 22, no. 12, pp. 5395–5407, 2013.
- [9] Z. Wang, S. Wang, J. Zhang, S. Wang, and S. Ma, “Probabilistic decision based block partitioning for future video coding,” *IEEE Transactions on Image Processing*, vol. 27, no. 3, pp. 1475–1486, 2018.
- [10] W. Kuang, Y.-L. Chan, S.-H. Tsang, and W.-C. Siu, “Online-learning-based bayesian decision rule for fast intra mode and CU partitioning algorithm in HEVC screen content coding,” *IEEE Transactions on Image Processing*, vol. 29, pp. 170–185, 2020.

TABLE III: Geometrically distributed symbols: comparison of average number of accesses needed for updating the array of cumulative counts

K	parameter of distribution	standard approach			ring-buffer approach	
		best case	worst case	ring-buffer approach		
		$E[X] = \frac{p}{1-p}$	$\frac{E[X]}{K} \cdot K$	$\frac{K - E[X]}{K} \cdot K$	$E[D] = \frac{2 \cdot p}{1-p^2}$	$\frac{E[D]}{K} \cdot K$
2	0	0.5	1	$1/2 \cdot K$	$4/3$	$2/3 \cdot K$
4	0	0.5	1	$1/4 \cdot K$	$4/3$	$1/3 \cdot K$
8	0	0.5	1	$1/8 \cdot K$	$4/3$	$1/6 \cdot K$
16	0	0.5	1	$1/16 \cdot K$	$4/3$	$1/12 \cdot K$
32	1	$1/\sqrt{2}$	2.4142	$0.0754 \cdot K$	2.8284	$0.0884 \cdot K$
64	2	$1/\sqrt[4]{2}$	5.2852	$0.0826 \cdot K$	5.7420	$0.0897 \cdot K$
128	3	$1/\sqrt[8]{2}$	11.0488	$0.0863 \cdot K$	11.527	$0.0901 \cdot K$
256	4	$1/\sqrt[16]{2}$	22.587	$0.0882 \cdot K$	23.076	$0.0901 \cdot K$
512	5	$1/\sqrt[32]{2}$	45.668	$0.0892 \cdot K$	46.163	$0.0902 \cdot K$
1024	6	$1/\sqrt[64]{2}$	91.833	$0.0900 \cdot K$	92.331	$0.0902 \cdot K$

- [11] Z. Chen, J. Shi, and W. Li, “Learned fast HEVC intra coding,” *IEEE Transactions on Image Processing*, vol. 29, pp. 5431–5446, 2020.
- [12] M. Saldanha, G. Sanchez, C. Marcon, and L. Agostini, “Complexity analysis of VVC intra coding,” in *2020 IEEE International Conference on Image Processing (ICIP)*, 2020, pp. 3119–3123.
- [13] M. Wang, S. Wang, J. Li, L. Zhang, Y. Wang, S. Ma, and S. Kwong, “Low complexity trellis-coded quantization in versatile video coding,” *IEEE Transactions on Image Processing*, vol. 30, pp. 2378–2393, 2021.
- [14] S. Liu, S. Cui, T. Li, H. Liu, Q. Yang, and H. Yang, “Fast CU partition algorithm based on swin-transformer for depth intra coding in 3D-HEVC,” *Multimedia Tools and Applications*, 2024.
- [15] F. Pakdaman, M. A. Adelimanesh, M. Gabbouj, and M. R. Hashemi, “Complexity analysis of next-generation VVC encoding and decoding,” in *2020 IEEE Int. Conf. on Image Proc. (ICIP)*, 2020, pp. 3134–3138.
- [16] A. Mercat, A. Mäkinen, J. Sainio, A. Lemmetti, M. Viitanen, and J. Vanne, “Comparative rate-distortion-complexity analysis of VVC and HEVC video codecs,” *IEEE Access*, vol. 9, pp. 67 813–67 828, 2021.
- [17] Y.-H. Chen and V. Sze, “A deeply pipelined CABAC decoder for HEVC supporting level 6.2 high-tier applications,” *IEEE Trans. on Circuits and Systems for Video Technology*, vol. 25, no. 5, pp. 856–868, 2015.
- [18] Y. Zhang and C. Lu, “A highly parallel hardware architecture of table-based CABAC bit rate estimator in an HEVC intra encoder,” *IEEE Transactions on Circuits and Systems for Video Technology*, vol. 29, no. 5, pp. 1544–1558, 2019.
- [19] F. L. L. Ramos, A. V. P. Saggiorato, B. Zatt, M. Porto, and S. Bampi, “Residual syntax elements analysis and design targeting high-throughput HEVC CABAC,” *IEEE Transactions on Circuits and Systems I: Regular Papers*, vol. 67, no. 2, pp. 475–488, 2020.
- [20] Y. Cai, Y. Fan, L. Huang, X. Zeng, H. Yin, and B. Zeng, “A fast CABAC hardware design for accelerating the rate estimation in HEVC,” *IEEE Transactions on Circuits and Systems for Video Technology*, vol. 32, no. 4, pp. 2385–2395, 2022.
- [21] J. Rissanen and G. Langdon, “Arithmetic coding,” *IBM Journal of Research and Development*, vol. 23, pp. 149 – 162, March 1979.
- [22] G. N. Martin, “Range encoding: An algorithm for removing redundancy from a digitized message,” in *Video & Data Recording Conference*, vol. 245, Southampton, UK, July 1979.
- [23] J. Duda, “Asymmetric numeral systems: entropy coding combining speed of Huffman coding with compression rate of arithmetic coding,” 2014. [Online]. Available: <https://arxiv.org/abs/1311.2540>
- [24] A. Moffat and M. Petri, “Large-alphabet semi-static entropy coding via asymmetric numeral systems,” *ACM Trans. Inf. Syst.*, vol. 38, no. 4, Jul. 2020.
- [25] T. Strutz, “Rescaling of symbol counts for adaptive rANS coding,” in *31st European Signal Processing Conference (EUSIPCO)*, Helsinki, Finland, September 2023, pp. 585 – 589.
- [26] Q. Sheng, H. Zhu, H. Sheng, X. Huang, J. Jiang, and C. Lai, “High efficiency lossless image recompression algorithm with asymmetric numeral systems for real-time mobile application,” *Journal of Real-Time Image Processing*, vol. 20, no. 5, p. 90, 2023.
- [27] D. Marpe, H. Schwarz, and T. Wiegand, “Context-based adaptive binary arithmetic coding in the H.264/AVC video compression standard,” *IEEE Transactions on Circuits and Systems for Video Technology*, vol. 13, no. 7, pp. 620–636, 2003.
- [28] V. Sze and M. Budagavi, “High throughput CABAC entropy coding in HEVC,” *IEEE Transactions on Circuits and Systems for Video Technology*, vol. 22, no. 12, pp. 1778–1791, 2012.
- [29] E. Belyaev, A. Turlikov, K. Egiazarian, and M. Gabbouj, “An efficient adaptive binary arithmetic coder with low memory requirement,” *IEEE Journal of Selected Topics in Signal Processing*, vol. 7, no. 6, pp. 1053–1061, 2013.
- [30] F. Aulí-Llinàs, P. Enfedaque, J. C. Moure, and V. Sanchez, “Bitplane image coding with parallel coefficient processing,” *IEEE Transactions on Image Processing*, vol. 25, no. 1, pp. 209–219, 2016.
- [31] S. Kim, B. Jo, S. Beack, T. Lee, and D. Jun, “Dynamic bit-plane arithmetic coding method for quantized spectral coefficients in USAC,” *IEEE Journal of Selected Topics in Signal Processing*, pp. 1–10, 2025.
- [32] J. Han and Y. Xu, “Probability model estimation for m-ary random variables,” in *2022 IEEE International Conference on Image Processing (ICIP)*, 2022, pp. 3021–3025.
- [33] Y. Chen, D. Murtherjee, J. Han, A. Grange, Y. Xu, Z. Liu, S. Parker, C. Chen, H. Su, U. Joshi, C.-H. Chiang, Y. Wang, P. Wilkins, J. Banksoski, L. Trudeau, N. Egge, J.-M. Valin, T. Davies, S. Midtskogen, A. Norkin, and P. de Rivaz, “An overview of core coding tools in the AV1 video codec,” in *2018 Picture Coding Symposium (PCS)*, 2018, pp. 41–45.
- [34] T. Strutz and P. Möller, “Screen content compression based on enhanced soft context formation,” *IEEE Transactions on Multimedia*, vol. 22, no. 5, pp. 1126–1138, 2020.
- [35] M. Chen, H. Su, S. Deng, and Y. Xu, “Machine learning based symbol probability distribution prediction for entropy coding in AV1,” in *2020 IEEE International Conference on Image Processing (ICIP)*, 2020, pp. 3374–3378.
- [36] D. E. O. Tzamarias, K. Chow, I. Blanes, and J. Serra-Sagristà, “Fast run-length compression of point cloud geometry,” *IEEE Transactions on Image Processing*, vol. 31, pp. 4490–4501, 2022.
- [37] H. Och, S. R. Uddehal, T. Strutz, and A. Kaup, “Enhanced color palette modeling for lossless screen content compression,” in *ICASSP 2024 - 2024 IEEE International Conference on Acoustics, Speech and Signal Processing (ICASSP)*, 2024, pp. 3670–3674.
- [38] M. P. Krishnan, L. Zhao, Z. Dong, T. Liu, W. Kuang, M. Tang, and S. Liu, “Enhanced frame context initialization for video coding beyond AV1,” in *2025 IEEE International Conference on Image Processing (ICIP)*, 2025, pp. 1594–1599.
- [39] A. Moffat, “An improved data structure for cumulative probability tables,” *Software: Practice and Experience*, vol. 29, no. 7, pp. 647–659, 1999.
- [40] T. Strutz and N. Schreiber, “Investigations on algorithm selection for interval-based coding methods,” *Multimedia Tools and Applications*, July 2025.
- [41] P. Fenwick, “A new data structure for cumulative probability tables,” *Software: Practice and Experience*, vol. 24, no. 3, pp. 327–336, March 1994.
- [42] I. Witten, R. Neal, and J. Cleary, “Arithmetic coding for data compression,” *Communications of the ACM*, vol. 30, pp. 520 – 540, Juni 1987.
- [43] Microsoft, “`__rdtsc`,” Available: <https://learn.microsoft.com/en-us/cpp/intrinsics/rdtsc?view=msvc-170>, accessed 23 April 2025.
- [44] T. Strutz, “Data files for testing entropy coding software,” 2025. [Online]. Available: <https://dx.doi.org/10.21227/40cv-tz15>
- [45] A. Said, “Comparative analysis of arithmetic coding computational complexity,” in *Data Compression Conference, 2004. Proceedings. DCC 2004*, 2004, p. 562, also: techn. report at HP Laboratories Palo Alto, HPL-2004-75.



Tilo Strutz holds a Dipl.-Ing. in Electrical Engineering (1994), Dr.-Ing. in Signal Processing (1997) and Dr.-Ing. habil. in Communications Engineering (2002) from the University of Rostock, Germany, where he mainly worked on problems of wavelet-based image compression. From 2003 to 2007, he worked at the European Molecular Biology Laboratory (Hamburg branch) in the field of multidimensional signal processing and data analysis. He was then Professor of Information and Coding Theory at the Leipzig University of Telecommunications (HfTL) until 2022. Tilo Strutz is now Professor of Image Processing and Computer Vision at Coburg University of Applied Sciences. His research interests range from general signal processing and special problems in image processing to data compression and machine learning.



Roman Rischke received the M.Sc. degree in business mathematics from Technische Universität Berlin, Germany, in 2012, and the Dr.rer.nat. degree in mathematics from Technische Universität München, Germany, in 2016. He worked as a Post-Doctoral Researcher with the Department of Artificial Intelligence, Fraunhofer Heinrich Hertz Institute, Berlin, and is now Professor of Data Science at Coburg University of Applied Sciences. His research interests include discrete optimization under data uncertainty, efficient and robust machine learning,

and federated learning.